CrystEngComm

COMMUNICATION

View Article Online
View Journal | View Issue

Cite this: *CrystEngComm*, 2015, **17**, 6852

Received 26th February 2015,
Accepted 1st April 2015

DOI: 10.1039/c5ce00398a

www.rsc.org/crystengcomm

Synthesis of size-controlled PtCu@Ru nanorattles *via* Pt seed-assisted formation of size-controlled removable Cu template†

Suhyun Park,‡[a] Donghwan Yoon,‡[a] Hionsuck Baik*[b] and Kwangyeol Lee*[a]

A facile synthetic strategy has been developed for size-controlled PtCu@Ru nanorattles *via* co-decomposition of Ru and Cu precursors in the presence of Pt nanoparticles. The presence of Pt nanoparticles induces a fast decomposition of Cu precursors, leading to the growth of the Cu phase on the Pt seeds. The Pt nanoparticle surface is partially alloyed with the Cu phase to form a PtCu alloy phase. Subsequent decomposition of Ru precursors leads to the formation of the Ru shell. The Cu layer between the core and shell of the intermediate PtCu@Cu@Ru nanoparticle, generated as a kinetic product, is then *in situ* removed by a CTAB (cetyltrimethylammonium bromide)-induced destabilization process to yield a novel nanorattle structure with a Pt-based core and a porous Ru shell. The diameter of the Ru shell could be conveniently controlled by varying the ratio of employed Cu and Ru precursors.

Hollow metallic nanocages or nanoframes with an inherently high surface area are receiving great attention due to their potential catalytic applications in important technological fields such as fuel cells[1–3] and electrocatalytic water splitting reactions.[4–6] Various methodologies are being actively sought to prepare hollow nanostructures with desirable compositions and structural features, and the common synthetic scheme invariably involves the formation of a shell or framework on the surface of a removable template and subsequent removal of the template by etching.[7–10] Therefore, the dimensional control of removable template nanoparticles is crucial for the size control of the final hollow or frame nanostructures. The size of hollow or frame nanostructures might have to be fine-tuned because the electrocatalytic conversion is greatly affected by the interaction between the catalytic system and electrode surface.[11–13] We have recently reported a facile one pot synthesis of Ru nanocages by co-decomposition of Ru and Cu, which involves *in situ* formation of a Cu@Ru core–shell and subsequent Cu phase removal, and its usage in oxygen evolution reaction.[14] However, the size control of the catalytic Ru nanocage was possible only for a certain size range, namely around 23.5 ± 2.5 nm. The size control of the *in situ* formed Cu nanotemplate has proved to be very challenging because the size of a Cu nanoparticle is determined by a delicate balance between the Cu growth and Ru-induced impediment of Cu growth. The size control of the nanocage was further complicated by the competing Cu phase dissolution.

We noted in several cases that the formation of nanocrystals from decomposing precursors can be greatly facilitated by the presence of heterophase seed nanocrystals.[15–22] In the presence of a suitable nanocrystalline seed, the decomposition of template precursors can result in a complete consumption of the precursors. Subsequent deposition of the catalytic metals on the nanotemplate, followed by dissolution of the template, would result in size-controlled hollow cages. This points to an idea that, in the presence of seeds, the *in situ* formed Cu nanocrystal templates might be size-controlled to eventually give size-controlled hollow cages as shown in Scheme 1. In order to test our idea, we studied the decomposition of Cu and Ru precursors in the presence of Pt

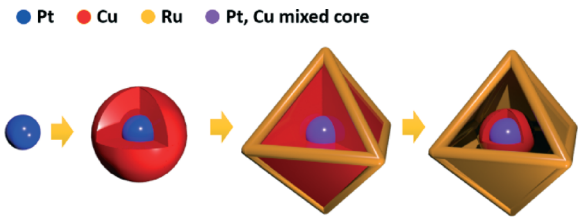

Scheme 1 Schematic synthetic strategy for size-controlled PtCu@Ru nanorattles. The Ru frame size is determined by the thickness of Cu layer. Violet core in final product denotes the partial surface alloying between Cu and Pt phases.

[a] *Department of Chemistry and Research Institute for Natural Sciences, Korea University, Seoul 136-701, Korea. E-mail: kylee1@korea.ac.kr; Tel: +82 2 3290 3139*
[b] *Korea Basic Science Institute (KBSI), Seoul 136-713, Korea. E-mail: baikhs@kbsi.re.kr*

† Electronic Supplementary Information (ESI) available. See DOI: 10.1039/c5ce00398a

‡ These authors contributed equally.

nanocrystal seeds at varying {Cu, Ru}/Pt ratios. Herein, we report an unprecedented size-controlled synthesis of Ru nanocages containing a PtCu rattle core.

A typical synthesis begins with the preparation of spherical Pt nanoparticles by decomposing $Pt(acac)_2$ (0.02 mmol, Aldrich, 97%) in oleylamine (15 mmol, Aldrich, 70%) at 200 °C for 5 min under 1 atm CO gas. The TEM image of synthesized Pt seed nanoparticles is shown in Fig. S1.† The average size was around 6.3 ± 0.8 nm. Pt seed nanoparticles (0.4 mg) dissolved in 1 mL of oleylamine were added in a slurry of $Cu(OAc)_2$ (0.02 mmol, Aldrich, 98%), $Ru(acac)_3$ (0.02 mmol, Strem Chemicals, 99%), CTAB (0.02 mmol, Aldrich, 99%), and 4 mL of oleylamine (12 mmol, Aldrich, 70%), prepared in a 100 mL Schlenk tube. The Schlenk tube, evacuated and then charged with 1 atm CO gas, was heated at 280 °C for 20 min. To the cooled solution, a mixture of toluene and methanol (v/v = 1/2) was added to give dark precipitates, which were further purified by centrifugal separation. Representative transmission electron microscope (TEM) images, X-ray powder diffraction (XRD) pattern, and high-resolution TEM (HRTEM) analysis are shown in Fig. 1. The octahedral nanorattles are highly uniform with an average size of 15.1 ± 1.1 nm (see ESI† Fig. S2 for detailed size analysis). The monodisperse size distribution and the structural feature of PtCu@Ru nanorattles are clearly demonstrated in Fig. 1a. The XRD data

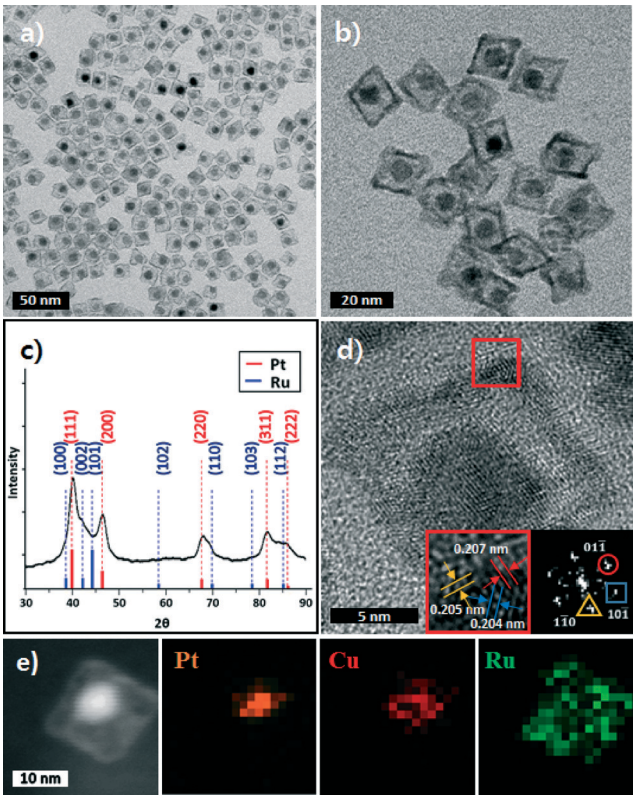

Fig. 1 a) TEM and b) HRTEM images of PtCu@Ru nanorattles. c) XRD pattern of PtCu@Ru nanorattles. d) HRTEM image with zone axis [111] and its FFT pattern. e) STEM image and elemental mapping data. The atomic compositions are found to be 17.9% Pt, 29.7% Cu and 52.4% Ru.

and fast Fourier transformation (FFT) patterns show the *hcp* (hexagonal close packing) atomic structure of Ru and *fcc* (face-centred cubic) atomic structure of Pt. XRD diffraction peaks of the Cu phase, which has a smaller atomic number, could not be easily identified.

The atomic compositions of PtCu@Ru nanorattle are found to be 17.9% Pt, 29.7% Cu, and 52.4% Ru. When compared to previously reported Cu-doped Ru nanocages,[14] a more substantial amount of Cu appears to remain. However, the elemental distribution of PtCu@Ru nanorattles obtained by EDX mapping in Fig. 1e shows distinct Pt and Cu signals from the core and the Ru signal from the shell (see ESI† Fig. S3a). Closer examination of the elemental compositions of the core shows that the Pt core is surrounded by the Cu layer. The incomplete Cu removal might have resulted from the alloying between surface Pt and Cu layer on the core Pt. Theoretically, Pt and Cu can easily mix to form a binary alloy system due to the negative mixing enthalpy of formation of Pt and Cu.[23,24] It is notable that the shell is nearly completely devoid of the Cu component. This seems to indicate that the mixing between Cu and Ru is minimal, plausibly due to the sequential deposition of Cu phase and Ru phase and due to the incompatibility between *hcp* Ru and *fcc* Cu.[25,26] HRTEM also reveals a highly polycrystalline Ru-based shell and a single crystalline Pt-based core. The lattice distances of $(01\bar{1})$, $(10\bar{1})$ and $(1\bar{1}0)$ planes were measured to be 0.207 nm, 0.204 nm, 0.205 nm, respectively, with a zone axis of [111].

The structural evolution of the PtCu@Ru nanorattles was studied by examining the temporal images of reaction intermediates in order to understand the detailed mechanism. At the initial stage of reaction (3 min), Cu atoms deposit on a Pt seed to form a core–shell structure. At this point, most nanocrystals have the Pt@Cu core–shell structure as shown in Fig. 2b, but the octahedral shape is not fully developed. Atomic compositions of Pt@Cu core–shell nanoparticles are found to be 91.3% Cu and 8.2% Pt. The content of Ru has been estimated under the detection limit (0.5%) (see ESI† Fig. S3b). As reaction proceeds, Ru deposits on the Pt@Cu core–shell nanoparticles to form a PtCu@Cu@Ru intermediate structure and develops into an octahedron shape. Bromide ions in CTAB can act as an etchant for the Cu phase, but can also control the Cu nanoparticle morphology.[14] The Cu layer between the core and shell of the PtCu@Cu@Ru intermediate diffuses out by the action of the CTAB intermediate. The hollowing-out process is completed in the reaction time of 20 min to finally give PtCu@Ru nanorattles. Further analyses of HR-TEM studies also confirm the nanorattle structure for the resulting nanostructure (see ESI† Fig. S4).

Interestingly, the core size gradually increases over time (see ESI† Fig. S5 for detailed size analysis). As discussed earlier, the formation of the Cu and Pt alloy phase is thermodynamically allowed,[23,24] and therefore the surface alloying between Pt and Cu explains the gradual size increase of the core.

The deposition of Ru occurs preferably on the edges rather than the facets, leading to the porous nature of the facet and

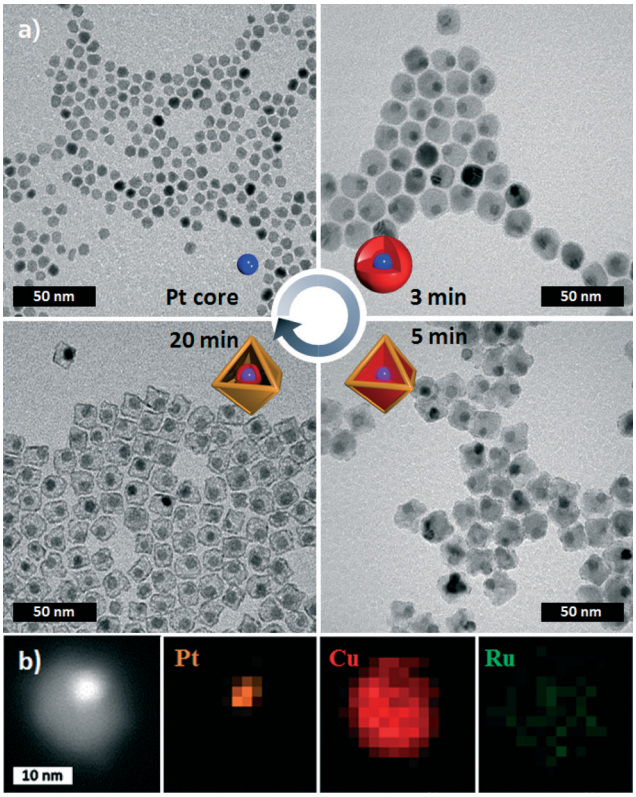

Fig. 2 a) TEM image of Pt core and temporal TEM images of reaction intermediates obtained at 3 minutes, 5 minutes and 20 minutes. b) STEM image and elemental mapping data of sample at 3 minutes. The atomic compositions are found to be 8.2% Pt and 91.3% Cu.

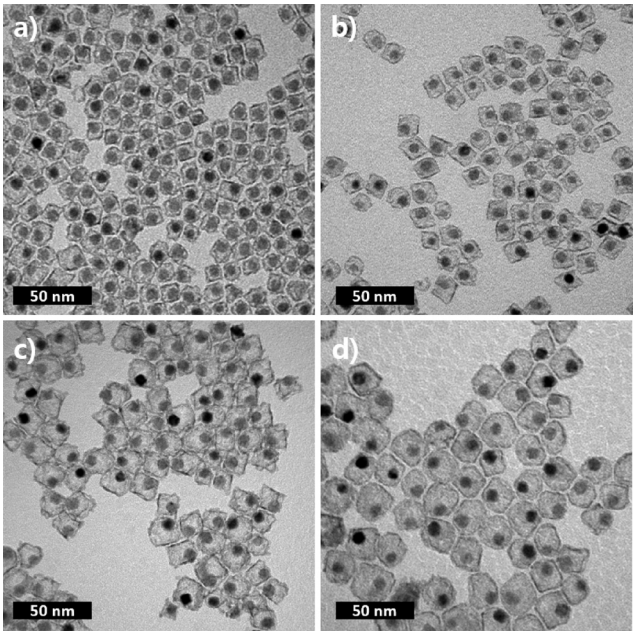

Fig. 3 TEM images of PtCu@Ru nanorattles with edge lengths of a) 13.4 nm, b) 15.1 nm, c) 16.7 nm and d) 19.8 nm, respectively, prepared from Cu/Ru ratios of 1.0, 1.0, 1.5, and 2.0.

subsequent leaching of the Cu content. The nanorattles are very robust under the reaction conditions; even after prolonged heating at 280 °C for 2 hours under CO gas, the nanostructures did not change. A number of heterostructures have been synthesized through the seed-mediated approach.[27–35] In many of these cases, the structure and shape of nanocrystal seeds play a key role in the nucleation and growth of the secondary metal. However, in our case, the morphology of the final product, PtCu@Ru nanorattle, seems to be mostly affected by the surfactant CTAB or CO gas rather than morphology of Pt seeds, since the spherical Pt nanoparticle without well-defined edges and vertices would have a minimal effect on the morphological evolution of the secondary metals (see ESI† Fig. S6).

The ratios of Cu/Pt and Cu/Ru are crucial factors in determining the overall size of the CuRu shell. The size of the PtCu@Ru nanorattle was tuned from 13.4 nm to 19.8 nm by controlling the amount of Pt seed (Fig. 3a), and by varying the amount of Cu precursor (Fig. 3b–d) as shown in Fig. 3 (see ESI† Fig. S7 for the size analysis). Nanorattle sizes of 13.4 nm, 15.1 nm, 16.7 nm, and 19.8 nm were obtained from Cu/Ru ratios of 1.0 (Fig. 3a), 1.0 (Fig. 3b), 1.5 (Fig. 3c) and 2.0 (Fig. 3d), with the amount of Pt seed nanoparticles fixed at 0.8 mg for Fig. 3a and at 0.4 mg for Fig. 3b–d (see ESI† Experimental section for details). The interior void space grew as the size of PtCu@Ru nanorattles increased, indicating that the interior void indeed results from the dissolution of the Cu phase. At a Cu/Ru ratio of 2.0, spherical shaped PtCu@Ru nanorattles with a size of 19.8 nm were obtained (Fig. 3d), indicating the limit of octahedral shape control by CTAB in fast Cu growth conditions. The ability to control the size of a hollow nanostructure has been rarely reported, although the size of the nanoparticle is closely linked to the overall catalytic performance. In this regard, herein reported size control of hollow nanostructures would be very useful in designing hollow structured nanocatalysts with optimal performance.

The oxidation states of Ru in PtCu@Ru nanorattles were analysed by X-ray photoelectron spectroscopy as shown in Fig. 4. The less intense Ru 3p signal was analysed instead of the main Ru 3d signal, as the latter is always obscured by the C 1s signal.[36] The peaks located at 484.5 eV, 486.7 eV, 462.2 eV and 464.2 eV could be assigned to Ru(0) $3p_{1/2}$, Ru(IV) $3p_{1/2}$, Ru(0) $3p_{3/2}$ and Ru(IV) $3p_{3/2}$, respectively (see ESI† Fig. S8). When compared to our previous report on Cu-doped Ru nanocages[14] the proportion of Ru(0) in the nanorattle is much larger in all four cases. The relative absence of the more easily oxidized Cu component in the Ru shell of the PtCu@Ru nanorattle has indeed preserved the Ru(0) state as compared to the case of Cu-doped Ru nanocages. Furthermore, the predominant Ru(0) component observed in the PtCu@Ru nanorattle is consistent with the physically detached PtCu core and the Ru shell. In the case of the Au/Cu_2O hollow sphere,[37] the high proportion of pure Au(0) in a hollow sphere observed by XPS data was used to confirm the binary nature of Au/Cu_2O nanocomposites. As the size of the PtCu@Ru nanorattle increased from 13.4 nm to 19.8 nm (Fig. 4), the component of Ru(0) in nanorattles gradually decreased. We suspect that the growth of large Cu

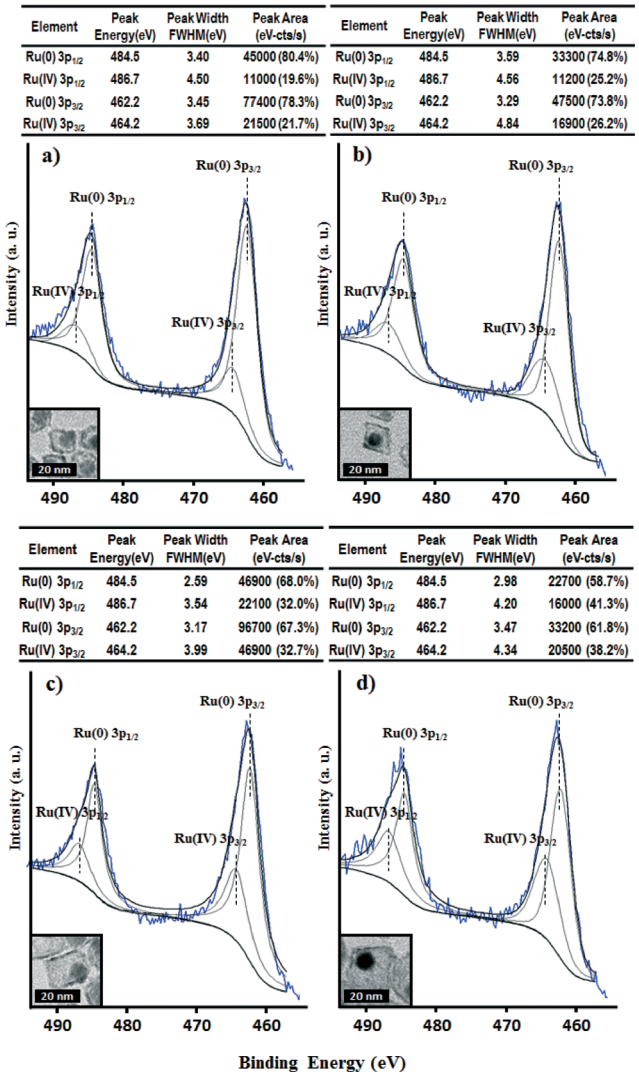

Fig. 4 X-ray photoelectron spectra of a) 13.4 nm, b) 15.1 nm, c) 16.7 nm, and d) 19.8 nm PtCu@Ru nanorattle.

nanoparticles is accompanied by the co-decomposition of a small amount of Ru species, although with slower decomposition kinetics. Higher CuRu alloy proportion in the final shell structure might contribute to the increased number of Ru species with higher oxidation states.

Conclusions

In summary, we have successfully synthesized size-controlled hollow octahedral nanocrystals in the presence of Pt seeds. The growth of the nanorattle structure is based on the fast nucleation of Cu on the preformed Pt nanoparticles. Subsequent deposition of the Ru phase and removal of Cu by the leaching effect of CTAB lead to the formation of a nanorattle. The mixing between Cu phase and Ru phase could be minimized, by completely decomposing the Cu phase assisted by the existing Pt seeds, to form the Ru phase shell, which is in contrast to the seedless co-decomposition of Cu and Ru precursors to form Cu-doped Ru hollow nanocages. The size of PtCu@Ru nanorattles could be conveniently controlled by varying the Cu/Ru ratio. The high surface area per mass of the hollow nanostructures would be greatly advantageous for the catalytic performance. Further studies are also underway to extend the synthetic concept to the preparation of size-controlled hollow nanostructures of other metals and alloys. It would be worthwhile to investigate the relationship between electrocatalytic performance and nanoparticle size. It would be also feasible to use multiply twinned seed nanocrystals in the fabrication of hollow structures with twinned shells; highly energetic structural features such as twinning boundary have been closely linked to the catalytic activity of nanoparticles.

Acknowledgements

This work was supported by the BioNano Health-Guard Research Centre funded by the Ministry of Science, ICT & Future Planning (MSIP) of Korea as Global Frontier Project H-GUARD_2013M3A6B2078946, NRF-2013R1A2A2A01015168, and NRF-20100020209. We thank KBSI for allowing the usage of their HRTEM instruments.

Notes and references

1 Z. Bai, L. Yang, L. Li, J. Lv, K. Wang and J. Zhang, *J. Phys. Chem. C*, 2009, **113**, 10568.
2 H. P. Liang, H. M. Zhang, J. S. Hu, Y. G. Guo, L. J. Wan and C. L. Bai, *Angew. Chem.*, 2004, **116**, 1566.
3 H. M. Chen, R. S. Liu, M. Y. Lo, S. C. Chang, L. D. Tsai, Y. M. Peng and J. F. Lee, *J. Phys. Chem. C*, 2008, **112**, 7522.
4 H. Zhou, E. M. Sabio, T. K. Townsend, T. Fan, D. Zhang and F. E. Osterloh, *Chem. Mater.*, 2010, **22**, 3362.
5 P. G. Hoertz and T. E. Mallouk, *Inorg. Chem.*, 2005, **44**, 6828.
6 S. W. Keller, S. A. Johnson, E. S. Brigham, E. H. Yonemoto and T. E. Mallouk, *J. Am. Chem. Soc.*, 1995, **117**, 12879.
7 N. A. Dhas and K. S. Suslick, *J. Am. Chem. Soc.*, 2005, **127**, 2368.
8 J. Liu, A. I. Maaroof, L. Wieczorek and M. B. Cortie, *Adv. Mater.*, 2005, **17**, 1276.
9 Y. Sun, B. Mayers and Y. Xia, *Adv. Mater.*, 2003, **15**, 641.
10 V. N. Phan, E.-K. Lim, T. Kim, M. Kim, Y. Choi, B. Kim, M. Lee, A. Oh, J. Jin, Y. Chae, H. Baik, J.-S. Suh, S. Haam, Y.-M. Huh and K. Lee, *Adv. Mater.*, 2013, **25**, 3202.
11 J. X. Wang, H. Inada, L. Wu, Y. Zhu, Y. Choi, P. Liu, W. P. Zhou and R. R. Adzic, *J. Am. Chem. Soc.*, 2009, **131**, 17298.
12 V. Mazumder, M. Chi, K. L. More and S. Sun, *J. Am. Chem. Soc.*, 2010, **132**, 7848.
13 J. Luo, L. Wang, D. Mott, P. N. Njoki, Y. Lin, T. He, Z. Xu, B. N. Wanjana, I.-I. S. Lim and C. J. Zhong, *Adv. Mater.*, 2008, **20**, 4342.
14 D. Yoon, S. Park, J. Park, J. Kim, H. Baik, H. Yang and K. Lee, *Nanoscale*, 2014, **6**, 12397.
15 M. Grzelczak, B. Rodriguez-González, J. Pérez-Juste and L. M. Liz-Marzán, *Adv. Mater.*, 2007, **19**, 2262.
16 C. Wang, S. Peng, R. Chan and S. Sun, *Small*, 2009, **5**, 567.

17 S. Xie, M. Jin, J. Tao, Y. Wang, Z. Xie, Y. Zhu and Y. Xia, *Chem. – Eur. J.*, 2012, **18**, 14974.
18 H. Gu, R. Zheng, X. Zhang and B. Xu, *J. Am. Chem. Soc.*, 2004, **126**, 5664.
19 J. Yoon, H. Baik, S. Lee, S. J. Kwon and K. Lee, *Nanoscale*, 2014, **6**, 6434.
20 Y. Vasquez, A. K. Sra and R. E. Schaak, *J. Am. Chem. Soc.*, 2005, **127**, 12504.
21 X. Xia, L. Figueroa-Cosme, J. Tao, H. Peng, G. Niu, Y. Zhu and Y. Xia, *J. Am. Chem. Soc.*, 2014, **136**, 10878.
22 J. Park, A. Oh, H. Baik, Y. S. Choi, S. J. Kwon and K. Lee, *Nanoscale*, 2014, **6**, 10551.
23 S. M. Foiles, M. I. Bakes and M. S. Daw, *Phys. Rev. B: Condens. Matter Mater. Phys.*, 1986, **33**, 7983.
24 S. Takizawa and K. Terakura, *Phys. Rev. B: Condens. Matter Mater. Phys.*, 1989, **39**, 5792.
25 L. Vitos, A. V. Ruban, H. L. Skriver and J. Kollár, *Surf. Sci.*, 1998, **411**, 186.
26 H. L. Skriver and N. M. Rosengaard, *Phys. Rev. B: Condens. Matter Mater. Phys.*, 1992, **46**, 7157.
27 Z. Peng, J. Wu and H. Yang, *Chem. Mater.*, 2010, **22**, 1098.
28 H. Kobayashi, B. Lim, J. Wang, P. H. C. Camargo, T. Yu, M. J. Kim and Y. Xia, *Chem. Phys. Lett.*, 2010, **494**, 249.
29 N. T. Khi, J. Yoon, H. Kim, S. Lee, B. Kim, H. Baik, S. J. Kwon and K. Lee, *Nanoscale*, 2013, **5**, 5738.
30 N. T. Khi, H. Baik, H. Lee, J. Yoon, J.-H. Sohn and K. Lee, *Nanoscale*, 2014, **6**, 11007.
31 N. T. Khi, J. Park, H. Baik, H. Lee, J.-H. Sohn and K. Lee, *Nanoscale*, 2015, **7**, 3941.
32 S. E. Habas, H. Lee, V. Radmilovic, G. A. Somorjai and P. Yang, *Nat. Mater.*, 2007, **6**, 692.
33 Y. Ding, F. Fan, Z. Tian and Z. L. Wang, *J. Am. Chem. Soc.*, 2010, **132**, 12480.
34 B. Sadtler, D. O. Demchenko, H. Zheng, S. M. Hughes, M. G. Merkle, U. Dahmen, L. W. Wang and A. P. Alivisatos, *J. Am. Chem. Soc.*, 2009, **131**, 5285.
35 J. H. Song, F. Kim, D. Kim and P. Yang, *Chem. – Eur. J.*, 2005, **11**, 910.
36 Z. Sun, Z. Liu, B. Han, S. Miao, Z. Miao and G. An, *J. Colloid Interface Sci.*, 2006, **304**, 323.
37 M. Pang, Q. Wang and H. C. Zeng, *Chem. – Eur. J.*, 2012, **18**, 14605.

